Journal of Applied Electrochemistry **31**: 897–903, 2001.

Electrodeposition and characterization of Au–Cu–Cd alloys

B. BOZZINI[1] and P.L. CAVALLOTTI[2]
[1]*INFM – Dipartimento di Ingegneria dell'Innovazione, Università di Lecce, v. Arnesano, I-73100 Lecce, Italy*
[2]*Dipartimento di Chimica Fisica Applicata, Politecnico di Milano, v. Mancinelli 7, I-20131, Milano, Italy*

Received 4 July 2000; accepted in revised form 29 January 2001

Key words: Au–Cu–Cd alloys, cyanide bath, electrodeposition, hydrodynamics, morphology

Abstract

The electrodeposition of Au–Cu–Cd alloys from cyanide baths was investigated under different hydrodynamic conditions. Alloys obtained at different current densities were characterized from the compositional, structural and morphological points of view. Depending on the electrodeposition current density, the deposit structure displays either one or two-phase disordered solid solutions; corresponding changes in mechanical properties were observed. Morphology and roughness show a marked smoothing transition when the current density is increased over the limit for the inception of Cu codeposition. The Cd^{2+} concentration in the bath is a critical factor for control of the electrodeposition process, especially in respect to compositional stability and absence of hydrogen incorporation. Alloy composition was shown to be critically affected by hydrodynamic conditions; strict control of flow conditions is needed in order to obtain alloys of desired and reproducible composition.

1. Introduction

The typical electroforming alloy for yellow 18 carat gold is Au–Cu–Cd deposited from free-cyanide baths. No industrially viable-processes are currently available which are not based on CN^- as a complexing agent and Cd as an alloying element empirically related to the enhancement of mechanical properties. Notwithstanding the extensive application of this alloy system, the available processes are not fully satisfactory because of compositional and mechanical inconsistencies of the electroplates. Process control is the single most critical issue. The lack of state-of-the-art electrochemical studies of the system leaves the industrial practice at a very rough empirical troubleshooting level.

Accurate but phenomenological studies were proposed in the seventies and early eighties [1–10]; more recent work is either very specific (pulse plating [11]) or markedly application-oriented [12]. The aim of the present work is to gain understanding of the electrochemical reasons for the observed compositional problems and to propose an original approach to industrial control of deposit uniformity.

As far as the baths are concerned, three main categories are known: (i) cyanoalkaline with Cd^{2+}–cyanide complexes, (ii) cyanoalkaline with organic Cd^{2+} complexes, (iii) sulphite. No scientific presentations of baths of type (iii) are available in the open literature and only some properties of the respective coatings have been reported [10]. Baths of kind (ii) are mainly described by patents: several very complex mixtures of polyoxyalkyl and aminophosphorus compounds are recommended. For a comprehensive list and patent literature see [2]. Scientific papers dealing with these baths [2, 4–9] discuss the properties of the coatings, but give no electrochemical details.

The behaviour of baths of type (i) is typical of a regular codeposition system: Cu content of the alloy tends to increase with increasing current density, temperature and stirring. The Cd content is only slightly affected by the operating conditions. Inconsistent conclusions regarding hydrodynamic effects have been reported [2, 11].

Use of organic Cd^{2+}-complexes does not really solve the industrial control problem; it tends to stabilise the Cd content of the coatings, which is not a critical issue. In contrast, control problems are increased in maintaining Cd^{2+} and organic additive concentrations in the bath.

Problems with baths of type (i) and (ii) are well known from practice and have also been reported in the literature [1, 2, 5]. The authors stress that these compositional instabilities are obtained from baths of perfectly controlled and stable composition under constant plating conditions. The typical problem is of a compositional nature and implies Au content and colour fluctuations. Compositional variations are present along the whole cross-section of the deposit, amounting to typically 40% of the Au content [2], but are particularly marked at the substrate-coating interface (1 to 2 μm) [2, 8].

Structural and morphological data are reported for ~18 carat deposits [5, 6, 9]. All authors agree that

a Au–Cu disordered solid solution is observed. One study [9] reports one such phase with a strong (111) preferred orientation and there is some doubtful evidence of a multi-phase structure with reflexions from four superlattice structures [5]. The cross-sectional growth morphology was reported to be either of the disoriented dispersion type with transition to field-oriented texture type [5] or lamellar [6].

2. Materials and methods

2.1. *Baths and electrochemical experiments*

Electrodeposition bath and operating conditions are given in Table 1. Electroplating and electrochemical measurements were carried out in a prismatic cell containing 300 cm^3 of solution equipped with a magnetic stirrer and in a RDE assembly in a beaker with thermostatic sheath, containing 500 cm^3 of solution. The relevant current density (c.d.) distribution and mass-transport characteristics were studied elsewhere [13]. The electrokinetic behaviour of these baths was characterized by linear sweep voltammetry (LSV) at a sweep rate of 0.5 mV s^{-1}. A Ag/AgCl RE was used, connected to the WE via a Piontelli probe in the prismatic cell, while potential data were corrected for IR drop in RDE experiments. The WEs were brass slabs metallographically polished using emery papers and lapped with γ-Al_2O_3 down to 1 μm. Brass slabs were coated with 15 to 20 μm of electroless Ni–P (P 9%) in some cases, for subsequent X-ray analyses. The counter electrode was a platinized Ti expanded mesh electrode. The electrodeposition experiments for the growth of cathodes to be employed in the HER studies were carried out galvanostatically with overpotential recording.

Table 1. Composition and operating conditions for the Au–Cu–Cd bath

Au (as $KAu(CN)_2$)	5 g l^{-1}
Cu (as $K_2Cu(CN)_3$)	50 g l^{-1}
$CdCO_3$	1.5 g l^{-1}
KCN	20 g l^{-1}
$KHCO_3$	7 g l^{-1}
K_2CO_3	5 g l^{-1}
T	70 °C
pH	10.5

2.2. *Structural and compositional investigations*

The crystalline structure of the plated alloys was studied by X-ray diffractometry with a powder goniometer. The surface morphology of the deposits was studied by SEM, AFM and laser interferometric profilometry. The quantitative composition analysis was performed by EDX. All the samples employed for structural and morphological studies had approximately the same thickness (±10%). Hydrogen release from the relevant electrodeposited materials was studied by the LECO gas-chromatographic technique, run with a temperature ramp from 100 to 800 °C at a scan rate of 0.6° s^{-1}.

3. Results and discussion

3.1. *LSV measurements*

LSV curves for baths of the kind reported in Table 1 are shown in Figure 1. These curves were recorded under natural convection conditions. Curves A and B refer to baths with Cd^{2+} 1.0 and 0.3 g dm^{-3}, respectively. The overall behaviour is typical for a regular

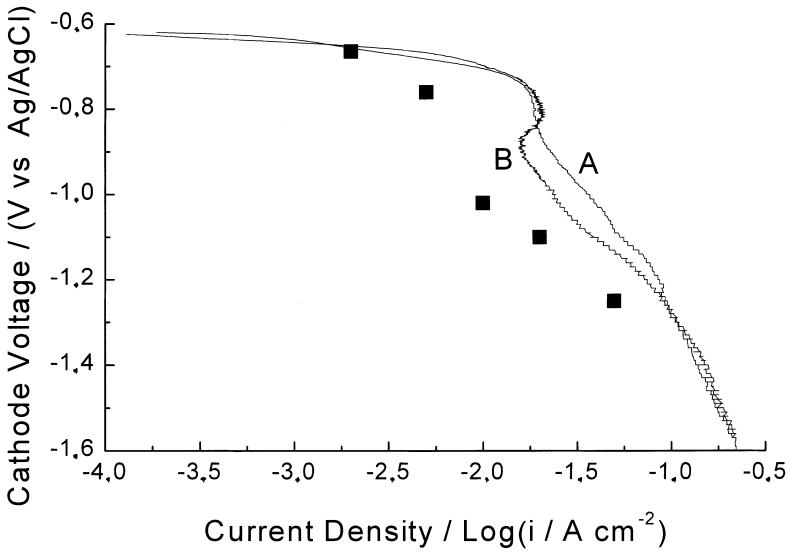

Fig. 1. Cathode linear sweep voltammograms for Au–Cu–Cd deposition from cyanoalkaline baths (see Table 1). Key: (A) Cd^{2+} 1.0 g l^{-1} (~6 wt % Cd in the alloy); (B) Cd^{2+} 0.3 g l^{-1} (~1.5 wt % Cd in the alloy), squares refer to steady-state (after 600 s) galvanostatic cathode voltages for Cd^{2+} 1.0 g l^{-1}.

codeposition system, with partial limiting c.d.'s for the main metals (Au^+ and Cu^+), this behaviour is confirmed by composition against c.d. data (see Figure 3). Curve B shows a cathode passivation peak which can be interpreted in terms of adsorption of nonelectroactive higher Cu^+-complexes, not affected by Cd, if this element is present in exceedingly low amounts [14].

3.2. *Galvanostatic measurements*

Steady-state electrodeposition overvoltages corresponding to galvanostatic runs are also reported in Figure 1, they are somewhat lower than the voltammetric ones; this behaviour may be due to the fact that the dynamic measurements are affected by the nucleation overvoltage. Deposition voltage transients of 10, 20, 50 and 100 min were recorded for a c.d. of 10 mA cm^{-2} under natural convection conditions; the common time intervals of the different transients overlap perfectly and show an almost linear increase of cathode voltage from -0.95 V vs Ag/AgCl to the steady state value of -1.1 V vs Ag/AgCl in approximately 20 min, after which the voltage does not show appreciable trends. This effect is linked to the build-up of the diffusion boundary layer thickness and respective cyanide and metal complex concentration gradients, which will be discussed in Section 3.4. The initial cathode potential variation is affected by mass-transport. Galvanostatic voltage transients were recorded for 20 min at three different magnetic stirrer rotation rates at 10 mA cm^{-2}. The relevant results are shown in Figure 2. At low rotation speeds the overvoltage is reduced at the beginning of the measurement, and a common voltage asymptote is gained when stagnant conditions are achieved, while at higher rotation speeds the mass-transport overvoltage is steadily lowered.

3.3. *Composition, current efficiency, mechanical properties and morphology as a function of current density*

Composition and current efficiency as a function of c.d. are shown in Figure 3. As expected for a regular codeposition system, the Au content and current efficiency are negatively correlated with the deposition c.d.; Cu tends to increase with c.d., while Cd content is little affected by deposition c.d. .

Crack-arrest fracture toughness and Milman plasticity index were measured by indentation methods according to a procedure described elsewhere [15]. The results are plotted as a function of electrodeposition c.d. in Figure 4. Fracture toughness tends to decrease systematically as Cu content increases and plasticity shows a minimum at the intermediate compositions.

X-ray diffraction results as a function of electrodeposition c.d. are shown in Figure 5. Disordered solid solutions are observed in all cases. One highly (1 1 1)-ordered Au-rich phase is obtained at low c.d.'s (2, 5 mA cm^{-2}). At intermediate c.d.'s (10, 20 mA cm^{-2}) two or three highly (1 1 1)-oriented phases appear: a Au-rich one and a Cu-rich one. In high-Cu deposits (50 mA cm^{-2}) one highly (1 1 1)-oriented phase prevails. Based on EDX evidence and c.d. distribution design of our cathodes, we can exclude that multiple phases are due to macroscopic compositional differences at different points of the coating sampled by the X-ray beam.

Roughness as a function of electrodeposition c.d. is shown in Figure 6 where both R_a and R_{rms} are reported. A sudden roughness drop is observed as composition changes from Au $\sim$100% (2 mA cm^{-2}) to $\sim$80% (5 mA cm^{-2}) and lower; subsequent c.d. rises correlate with an increase in roughness, as expected.

For the roughness transition at low c.d.'s, see also SEM and AFM imaging in Figures 7 and 8, respectively. The surface morphology of single-phase Au-rich deposits (2 mA cm^{-2}) consists of a granular structure with

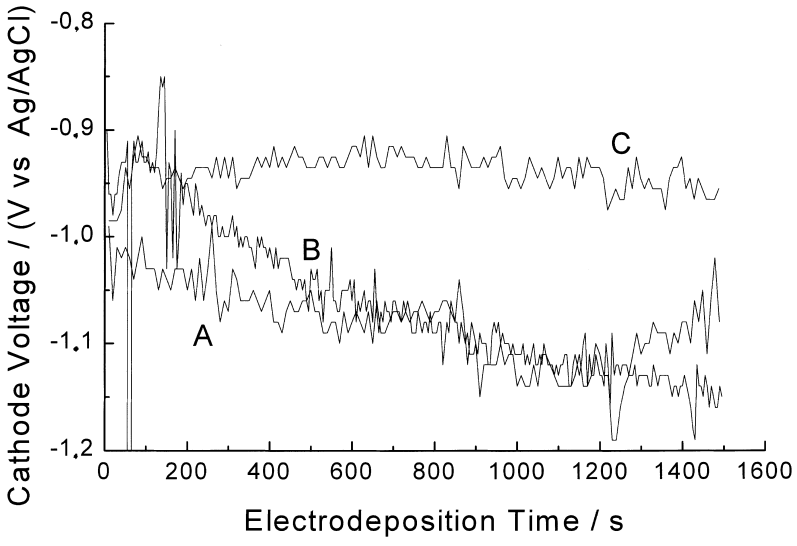

Fig. 2. Galvanostatic voltage transients for different stirrer bar rotation rates, c.d. 10 mA cm^{-2}.

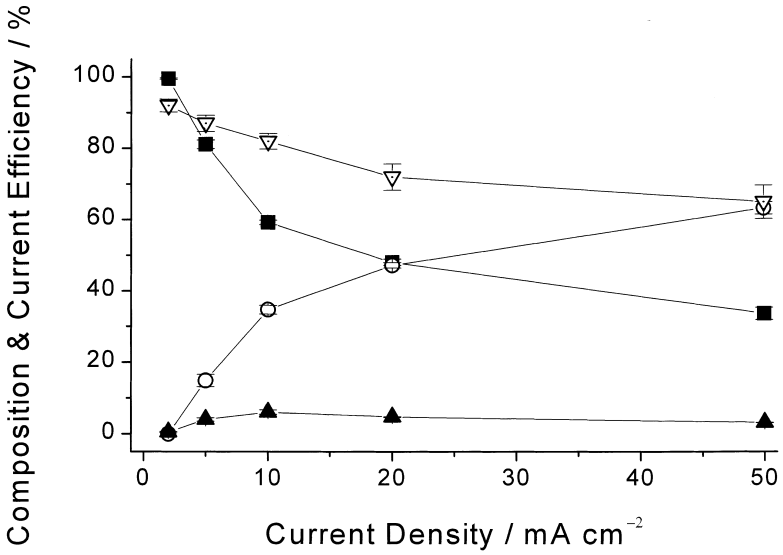

Fig. 3. Composition (EDX) and current efficiency as a function of c.d. Key: (■) Au, (○) Cu, (▲) Cd and (▽) η_{cath}.

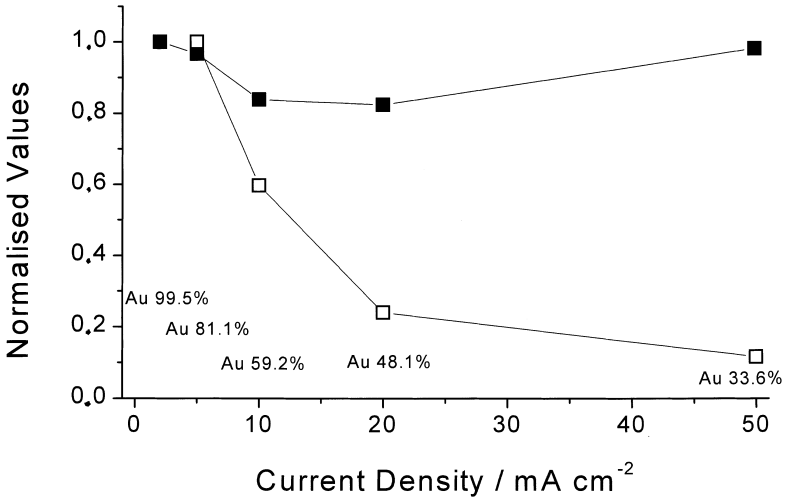

Fig. 4. Relative variations of crack-arrest fracture toughness K_{ICo} (□) and Milman plasticity index δ (■) as a function of c.d.

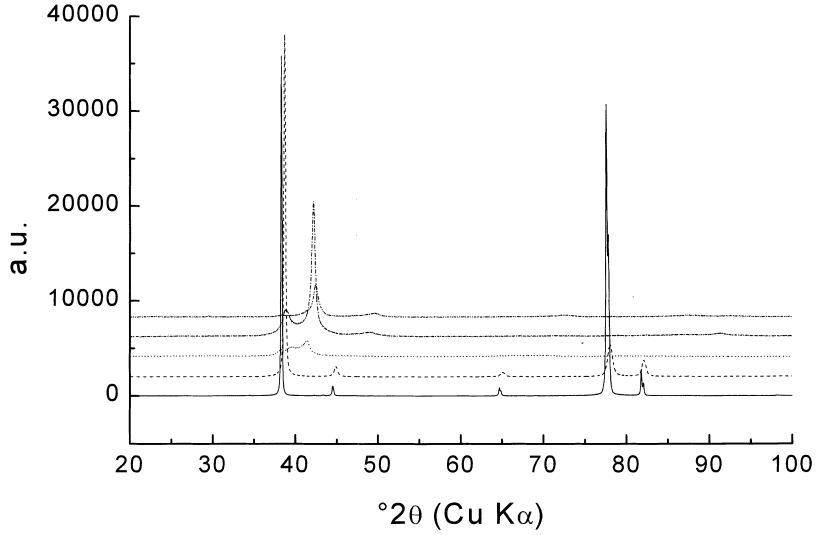

Fig. 5. Powder X-ray diffractograms of Au–Cu alloys electrodeposited at various c.d. Key: (——) 2, (- - - -) 5, (· · · · ·) 10, (– – – – –) 20 and (– · · – · · –) 50 mA cm^{-2}.

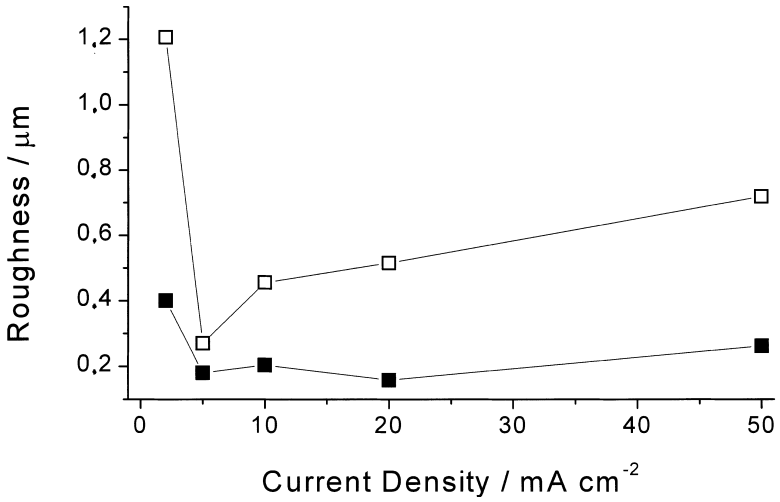

Fig. 6. Laser interferometry roughness measurements as a function of electrodeposition c.d. Key: (■) R_a and (□) R_{rms}.

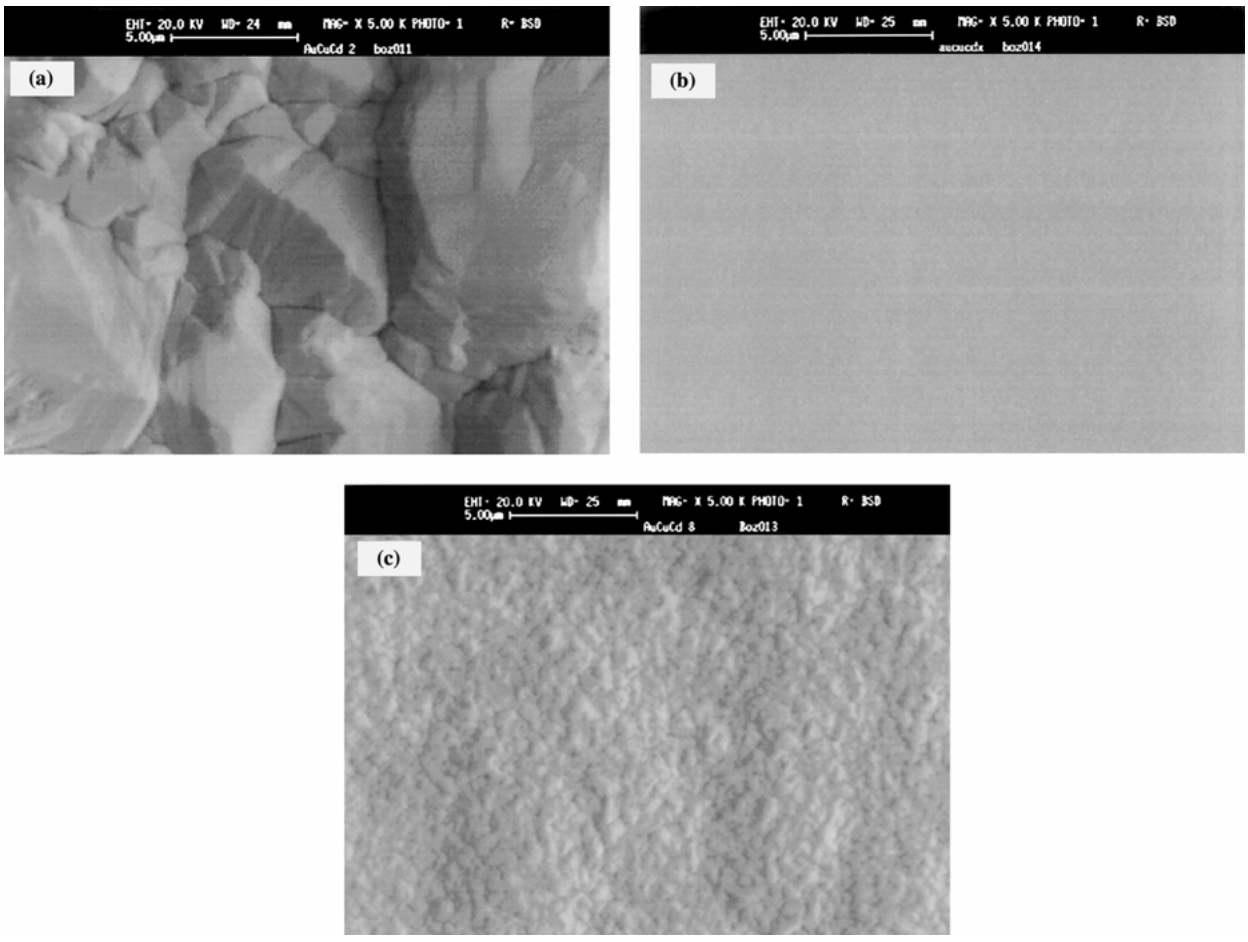

Fig. 7. SEM surface micrographs of Au–Cu–Cd deposits obtained at different c.d.: (a) 2, (b) 10 and (c) 20 mA cm^{-2}.

sharp ridges (Figure 7(a)). As soon as sizeable amounts of Cu are codeposited, a very smooth morphology is obtained (Figure 7(b)), which tends to grow unstable through formation of granular and powdery features at the highest investigated c.d.'s (Figure 7(c)). The morphology of extremely smooth deposits, obtained at intermediate c.d.'s, was investigated by AFM and shows the presence of tiny bumps ~10 to 20 nm high, which cannot be resolved by SEM (Figure 8).

LECO analyses show no measurable hydrogen incorporation from the bath containing the prescribed amount of Cd^{2+} (1 g dm^{-3}). If the Cd^{2+} concentration is too low (e.g., 0.3 g dm^{-3}) the LECO behaviour is the same as for Au–Cu alloys [16] with two desorption

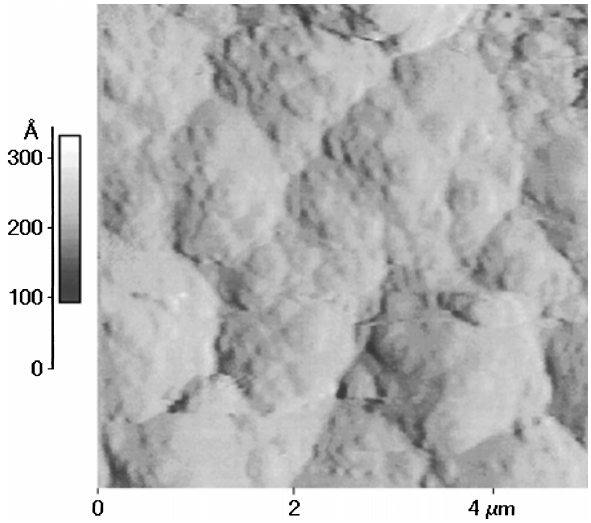

Fig. 8. AFM surface morphology (contact mode) of a deposit obtained at 10 mA cm^{-2}.

peaks: a large one (~1.3 dm^3 kg^{-1}) at ~450 °C and a smaller one (~0.1 dm^3 kg^{-1}) at ~670 °C.

3.4. *Dependence of composition on electrodeposition time and hydrodynamic conditions*

Compositional variations as a function of galvanostatic electrodeposition time under given hydrodynamic conditions were observed. The EDX composition of different samples grown for times in the range 1 to 100 min under natural convection conditions is shown in Figure 9. A steady increase in Au content is observed; the amount of codeposited Cd is not appreciably affected by the time of electrolysis.

Under given galvanostatic conditions and for a fixed electrodeposition time, deposit composition is affected by hydrodynamic conditions. RDE experiments with several cathode rotation rates are shown in Figure 10. Stagnant conditions give rise to low Au contents. If forced convection conditions are imposed, the composition rapidly increases towards an asymptotic value, which is, of course, a function of the electrodeposition time.

Cross sections of deposits obtained under different hydrodynamic conditions confirm this view. Natural convection brings about the formation of banded deposits, linked to the existence of local convection cells, which tend to grow richer in Au close to the substrate (Figure 11(a)). Coatings grown on the RDE show homogeneous composition with a Cu-rich induction layer (Figure 11(b)). A tentative explanation of these phenomena can be given considering the variation of the relative nobility of metal cations, especially Cu^+, because of CN^- buildup in the catholyte due to the decomplexing of reduced metal. CN^- removal is driven by mass-transport from the cathode into the bulk electrolyte. The observed decrease in Cu content with increasing electrodeposition time and mass-transport may be due to the fact that less noble higher cyanocomplexes form at high cathodic CN^- concentrations and, correspondingly, the Au content increases, while the Cd content is not markedly affected. This suggests that the compositional peculiarities of the Au–Cu–Cd alloy electrodeposition system are strongly affected by mass-transport effects. This finding can be used for the design of optimal electrodeposition conditions and cells.

4. Conclusions

The cyanide bath investigated shows a regular codeposition behaviour, seriously affected by mass transport; hydrodynamic effects and related transients have major compositional effects. The criticality of mass-transport conditions can be related to the build-up of metal-complex concentration gradients.

As far as the crystalline structure and mechanical properties are concerned, intermediate compositions are

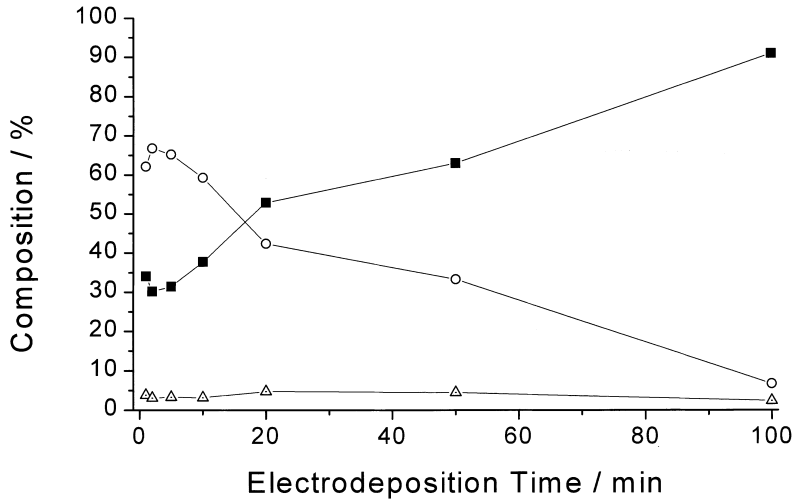

Fig. 9. Time dependence of composition (EDX) for different galvanostatic electrodeposition times (c.d. 10 mA cm^{-1}, natural convection with vertical cathodes, each point corresponds to a different sample plated independently). Key: (■) Au%, (○) Cu% and (△) Cd%.

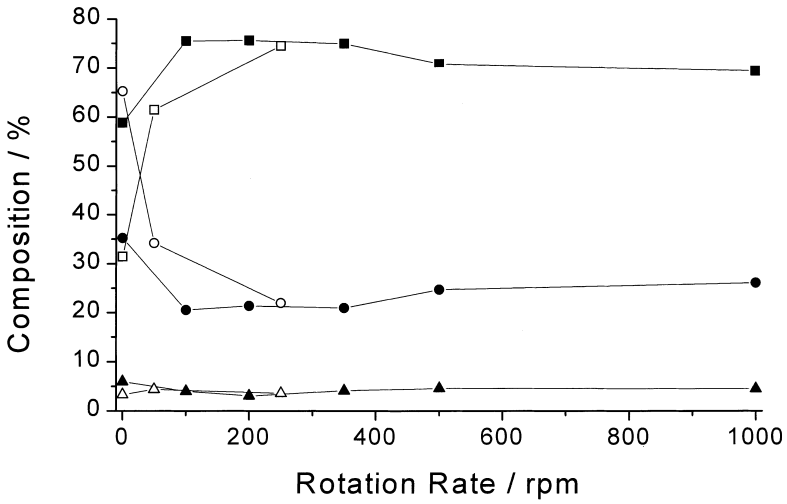

Fig. 10. Dependence of composition (EDX) for different RDE (■ Au%, ● Cu%, ▲ Cd%) or bar stirrer (□ Au%, ○ Cu%, △ Cd%) rotation rates (c.d. 10 mA cm^{-1}, electrodeposition time 30 min, each point corresponds to a different sample plated independently).

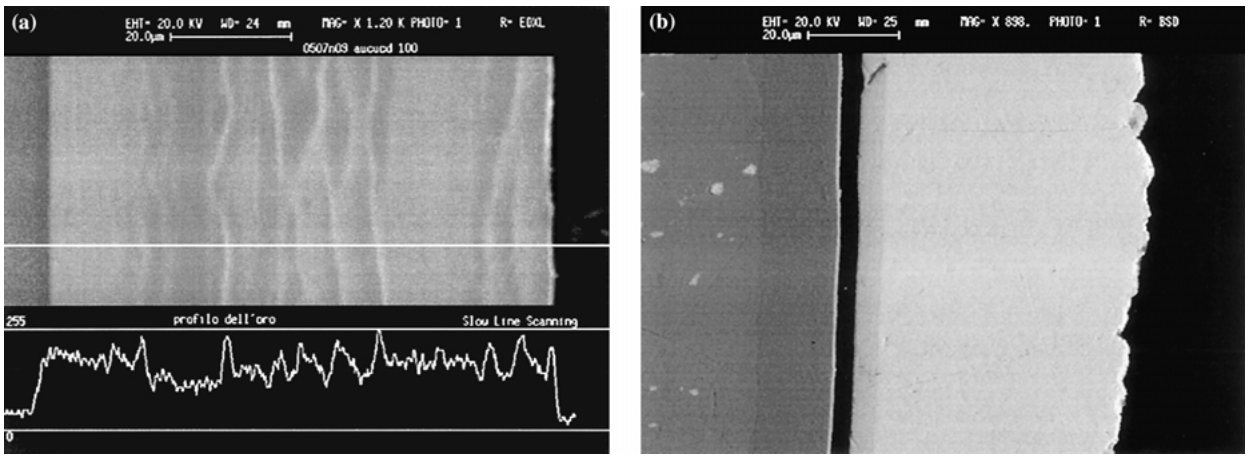

Fig. 11. SEM cross-sectional micrographs of Au–Cu–Cd deposits obtained at 10 mA cm^{-1}: (a) natural convection, 100 min, Au 90% (Au line scan is displayed at the bottom, substrate on the right-hand side); (b) RDE 500 rpm, 60 min, Au 68% (substrate on the right-hand side: from the right the following materials can be observed with different compositional contrasts: brass substrate, Ni–P interlayer, detachment due to metallographic polishing of the cross-section, Cu-rich induction layer, Au-rich layer).

related to two-phase disordered solid solutions displaying reduced plasticity; toughness correlates negatively with Cu content, irrespective of phase composition. Cu incorporation into the alloy is related to smoothing of the deposits.

Hydrogen incorporation, which is generally linked to deposit embrittlement, is controlled by Cd^{2+} concentration in the bath. If a critical threshold is exceeded, electrode kinetics are affected and no hydrogen incorporation takes place.

References

1. D.R. Mason and P. Wilkinson, *Galvano-Organo* **45** (1976) 651.
2. B. Inglot and J. Socha, *Galvanotechnik* **75** (1984) 1362.
3. B. Inglot and J. Socha, *Galvanotechnik* **75** (1984) 1528.
4. M. Dettke, R. Ludwig, K.U. Martin and W. Riedel, *Galvanotechnik* **62** (1971) 773.
5. M. Dettke, R. Ludwig, K.U. Martin and W. Riedel, *Galvanotechnik* **63** (1972) 729.
6. J.J. Robert, *Galvano-Organo* **46** (1976) 33.
7. J.J. Robert, *Galvano-Organo* **46** (1976) 114.
8. L. Chollet and J. Béguin, *Oberfläche-surface* **17** (1976) 168.
9. S. Steinmann, W. Flümann and W. Saxer, *Metalloberfläche* **29** (1975) 154.
10. W.A. Fairweather, *Gold Bull.* **10** (1977) 15.
11. A. Ruffoni and D. Landolt, *Electrochim. Acta* **33** (1988) 1273, 1281.
12. W. Saxer, *Galvanotechnik* **82** (1991) 3427.
13. B. Bozzini, G. Bollini, F. Pavan and P.L. Cavallotti, *Trans. IMF* **75** (1997) 175.
14. B. Bozzini, P.L. Cavallotti and G. Giovannelli, Proceedings of the 3rd international symposium on 'Electrocatalysis' (edited by S. Hocevar, M. Gaberscek and A. Pintar), Portoroz-Portorose (SLO) 1999, p. 190.
15. B. Bozzini, G. Giovannelli, M. Boniardi and P.L. Cavallotti, *Composites Sci. Technol.* **59** (1999) 1579.
16. B. Bozzini, P.L. Cavallotti and G. Giovannelli 'Fundamentals of Electrochemical Deposition and Dissolution', D. Landolt, M. Matlosz, Y. Sato eds., PV 99–33 Electrochemical Society Proceedings, pp. 81–100.